Modeling and simulation of sensor orientation errors in garments

Holger Harms
Wearable Computing Lab.
ETH Zurich
harms@ife.ee.ethz.ch

Oliver Amft
Wearable Computing Lab.
ETH Zurich
amft@ieee.org

Gerhard Tröster
Wearable Computing Lab.
ETH Zurich
troester@ife.ee.ethz.ch

ABSTRACT

We report in this paper on a novel modeling and simulation approach to predict orientation errors of garment-attached sensors and their effect on posture classification. Such errors occur frequently in smart garment implementations and can reduce sensor information quality for movement and posture recognition. A kinematic model of the human upper-body was developed to simulate upper limb postures and the output of virtual 3D acceleration sensors. The model was enhanced with a statistical approximation of garment-related orientation errors. We derived this model from acceleration sensor deviations between skin- and garment-attached units. The feasibility of our body model and the garment-attached sensor deviation was validated in experimental data. We compared the classification performance for ten posture types that are frequently used in shoulder rehabilitation. In a validation set of 7 participants we observed similar classifier confusions and a relative error of 2.6% (SD:±3.2%) between simulation and experiment. We utilized the model to estimate classification performance for further simulated textile error distributions. Our simulations showed that classification performance depends on low deviations of an acceleration sensor at the lower arm, while a sensor at the upper arm was less critical. Moreover, we included magnetic field sensors in our simulation. With the help of this additional modality our posture classification performance increased by 18%. We conclude that simulation of skin- and garment-attached sensors is a feasible approach to expedite design and development process of smart garments.

1. INTRODUCTION

Smart garments provide seamless integration of sensing and processing elements in textiles that enable new fields for personalized services and support [13]. Movement and posture monitoring is a vital application of smart garments. Various smart garment implementations have been proposed for this task, e.g. [2, 5, 7, 9, 18].

Especially for garments intended to be worn for a full day, unobtrusive fitting and attachment are essential prerequisites for wearer acceptance [6, 10]. Nevertheless, current smart garments used for movement and posture monitoring require a tight fit and precise alignment of garment-attached sensors to body parts [12,14,17]. While this setup is feasible and accepted for expert-supervised evaluations, tight fitting reduces wearing comfort. Moreover it cannot be maintained for unsupervised activity monitoring, as for example in unsupervised rehabilitation training of a patient.

While loose fitting garments [7] overcome these restrictions, they could record unreliable orientation data due changes in garment alignment relatively to the wearer's skin. Direction and displacement of alignment-changes depend on a number of aspects, including type and mechanical parameter of the garment, fitting, considered body position, and involved movements. First approaches to tackle sensor displacement have been proposed using heuristics and optimizations for sensor-derived features [11] and classifiers [8]. A description of garment-skin alignment for body postures has, to our knowledge, not been attempted. However, it would represent a vital basis to estimate sensor orientation errors. Information on these orientation errors allow to determine their impact in particular configurations of garments, fitting, and activities.

This paper provides the following contributions:

1. We introduce a combined model of upper limb kinematics and sensor operation, to simulate upper-body limb postures. The model was validated against human performance of shoulder and elbow postures covering five degrees of freedom (DOF).

2. A statistical model for predicting orientation errors of garment-attached sensors is introduced. We derived the model from orientation errors measured between acceleration sensor at body skin and the garment. In our evaluation of the model, we compared the rehabilitation posture classification of predicted and actual experimental data.

3. Using the validated models we present an exploratory analysis of classification performances for further simulated orientation error distributions. Moreover, we included a model of magnetic field sensors in our simulation and report on particular improvements achieved in combination with acceleration sensors.

Digital Object Identifier: 10.4108/ICST.BODYNETS2009.5977
http://dx.doi.org/10.4108/ICST.BODYNETS2009.5977

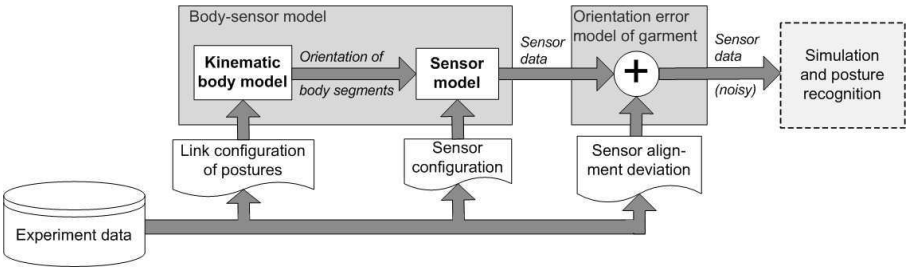

Figure 1: Approach to model and simulate body postures and garment-related orientation errors.

For our validation we selected postures from shoulder and elbow rehabilitation, since smart garments are a promising support tool in movement rehabilitation [7, 14].

2. TERMS AND OVERVIEW

In order to model and simulate garment-related alignment changes during postures we developed a two-step approach. In the first step a kinematic upper-body model was used to calculate the orientation of upper-limbs, given a parametric description of postures by joint angle configurations. Subsequently, these body segment orientations are translated into outputs of virtual sensors using according sensor models. This sensor model incorporates specific properties of a selected sensing modality, e.g. the operation concept of an acceleration sensor.

In a second step, an orientation error model was derived to describe garment-related alignment changes that affect attached sensors. The orientation error model is configurable as it depends on the garment fitting, type and position of sensors, and the intensity of expected movements. We used the orientation error model to modulate outputs of the previous body-sensor modeling step.

Figure 1 illustrates the individual modeling steps. The kinematic body model and the sensor modeling are described and validated in Section 3. The orientation error modeling is introduced and compared to experimental data in Section 4. Subsequently, we explored the influence of orientation errors on posture classification in Section 5 and introduced an additional sensor modality in the simulation in Section 6.

3. BODY-SENSOR MODEL

We present in this section our body-sensor modeling according to Figure 1. The model consists of a 3-dimensional kinematic model describing upper limbs orientations, and a sensor model, describing ideal sensor modality outputs. The complete body-sensor model was validated by comparing acceleration sensor readings from experimentally conducted postures to the simulation.

3.1 Kinematic body model

We modeled the upper-body anatomy as a system of linked body segments connected by rotational joints [1]. Starting point of the first link and reference point for all Cartesian coordinates is near the model's neck (T1 thoracic vertebra). Our model consists of seven serially connected links, describing five DOF of the right upper limb (see Table 1). While the

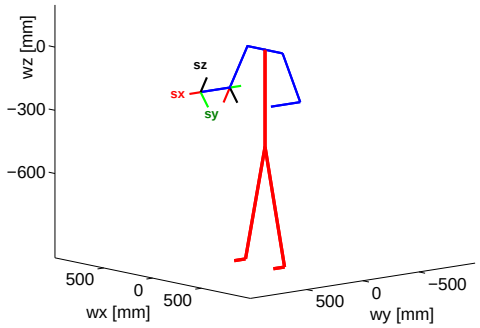

Figure 2: Sample configuration and resulting posture of the body model. Orientation vectors at the end of right upper arm and forearm ($\vec{sx}$,$\vec{sy}$,$\vec{sz}$) indicate the body segment orientations. The world coordinate axes (wx,wy,wz) are relative positions to the reference point at the neck.

right body side was sufficient for our shoulder and elbow posture evaluation the model description can be conveniently extended to the left body side as well. Body segments that represented limb parts were specified according to anthropometric measures of man (20-65 years, 78.4 kg) [16].

Resolving Cartesian coordinates and orientations of such serial-link manipulators is known as a forward kinematics problem. One common and computational inexpensive approach to forward kinematics is the expression of serial-link manipulators by description matrices [15]. These consist in the simplest case of a Denavit-Hartenberg (DH) parameter set (Θ, D, A, α), describing each link/joint pair as a coordinate transformation from the previous coordinate system to the next coordinate system [4]. Coordinate rotations are described by Θ (angle) and α (twist), translations correspond to D (offset) and A (length). The description matrices can be refined to include inertial and frictional parameters. However, in our work we limited the description of upper limb kinematics to the DH parameter set and assumed constant mass and mass distribution for all body segments.

Our implementation of the kinematic body model is based on the Robotics Toolbox [3], which provides basic kinematic operations for MATLAB. On top of this toolbox we modeled

Digital Object Identifier: 10.4108/ICST.BODYNETS2009.5977
http://dx.doi.org/10.4108/ICST.BODYNETS2009.5977

the upper-body using the serial-link manipulator with the DH parameter set, detailed in Table 1. Figure 2 illustrates a sample configuration of our body model, indicating body segments for upper arm and forearm, as well as the body segment-relative coordinate systems.

3.2 Sensor model

Subsequently we used body segment orientation information obtained with the kinematic body model to derive the output of acceleration sensors in a sensor model. For our purposes of describing statically adopted body postures, the static component of acceleration sensor responses was sufficient.

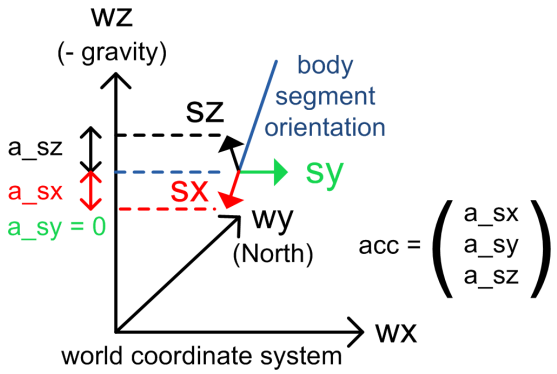

Figure 3: Derivation of acceleration sensor output ($\vec{acc}$) for body segments. Vectors $\vec{sx}$, $\vec{sy}$ and $\vec{sz}$ correspond to unit vectors along the body segment's coordinate system, a_sx, a_sy and a_sz indicate their projections on wz.

Sensor outputs were derived by considering the orientation of body segments relatively to world coordinates, see Figure 3. Given the body segment's orientation, we derived unit vectors ($\vec{sx}$, $\vec{sy}$, $\vec{sz}$) along each axis of its coordinate system and projected each vector on the z-axis (wz) of the world coordinate system. The length (and direction) of the three projections (a_sx, a_sy, a_sz) corresponds to each one output of an acceleration sensor axis with $-1g \leq acc \leq 1g$. In a similar way, we derived the outputs of magnetic field sensors by considering the projection on the world coordinate system's y-axis (which was North by convention).

3.3 Body-sensor model validation

In order to validate the body-sensor model, we analyzed the error between simulated and actual acceleration sensor readings for selected arm postures. We selected a set of five validation postures that specifically manipulate one DOF.

The experimental recordings were performed with acceleration sensors attached to the skin at forearm and upper arm from one male subject (28 years, body size of 182 cm).

The mean angular error for all postures was below 10°(9.5°for the upper arm, 6°for lower arm), which indicates the sufficient function of the body-sensor model and permits its use in subsequent analysis. The remaining angular errors were primarily caused by inaccurately adopted postures and limitations due to joint constraints. Moreover, body tissue and superficial muscles at the upper arm resulted in rotations of the attached sensor.

4. ORIENTATION ERROR MODEL

The body-sensor model provides body segment orientation information and can be used to simulate sensor outputs if the sensors are tightly coupled to body segments. With the additional model introduced in this section, we target a simulation of garment-related orientation errors. In this representation, the sensor relative orientation with respect to the body segment may change. We focused in this work on modeling orientation errors as a function of the garment fitting.

As outlined in Figure 1, the orientation error model is used to modulate simulated sensor outputs of the body-sensor model. Moreover, we present our validation of the combined body-sensor and orientation error models in a classification task.

4.1 Error modeling approach

We derived statistical approximations of the orientation error of garment-attached sensor outputs during posture performances. These approximations were obtained by computing the orientation deviation between simultaneous readings of skin- and garment-attached miniature acceleration sensors. We considered each sensor axis individually, since it can be affected by specific orientation errors. Moreover, we assumed that this error can be modeled, in its simplest form, by a Gaussian distribution. Hence, mean and standard deviation of orientation errors must be estimated for each sensor-axis of all considered sensors.

The Gaussian model approximation has the benefit that model parameters could be direct interpreted:

- Estimated mean of a Gaussian error model can be interpreted as an average orientation offset of garment-attached sensors relative to body segments. These means represent a constant offset of the sensor signal in all data, that consequenly do not affect our subsequent posture recognition. Therefore we omitted the mean component from our orientation error model.
- Standard deviation of Gaussian error models indicates a range of sensor orientations, in which the garment will disturb particular sensor axes. These orientation errors are assumed to be constant for the duration of every posture adopted during the repeated execution of posture exercises. Hence, this component is essential for the orientation error model. We hypothesize that the standard deviation could be interpreted as a metric describing garment fitting to a wearer. For the case of a tight-fitting garment the orientation of a sensor remains constant, resulting in a standard deviation close to zero. If a garment fits less tightly, it is more likely that a larger orientation error occurs and consequently results in a larger standard deviation in the error model.

Our approach has the following constraints and parameter, that need to be considered:

Digital Object Identifier: 10.4108/ICST.BODYNETS2009.5977
http://dx.doi.org/10.4108/ICST.BODYNETS2009.5977

Link	Twist α [rad]	Length A	Angle Θ [rad]	Offset D	Functional motion
1	0	length clavicle	0	0	N/A
2	$\pi/2$	0	0	0	Shoulder flexion/extension
3	0	0	$-\pi/2$	0	Shoulder adduction/abduction
4	$-\pi/2$	0	0	0	N/A
5	$\pi/2$	0	0	-(length upper arm)	Shoulder internal/external rotation
6	$-\pi/2$	0	0	0	Elbow flexion/extension
7	0	0	0	-(length forearm)	Forearm pronation/supination

Table 1: Denavit-Hartenberg (DH) parameter set of the link configuration used to calibrate the body-sensor model to exercise postures.

- The particular set of postures and intensity of movements influence orientation errors between body and garment-attached sensors. We focused in this work on a fixed posture set that is frequently considered in shoulder and elbow rehabilitation. A different set of postures would lead to different orientation errors. Postures that introduce a particularly high orientation error had been identified in earlier works [8].
- Different sensor modalities may incur independent errors for a set of postures. Sensors providing incomplete orientation information are potentially not sensitive to particular orientation errors. While this affects acceleration sensors that capture gravitational effects in our approach, acceleration serves well to recognize body postures.
- Garment natural fitting influences orientation errors. Hence, sensors in a garment that is tightly fitting may obtain no orientation errors, similar to body-attached sensors. We specifically considered this aspect by sampling orientation errors from actual posture performances of different wearers and body heights.

4.2 Error model implementation

We estimated garment-related orientation errors for two acceleration sensors attached to upper arm and forearm using the SMASH system [7]. The setup for the sensors at the forearm is shown in Figure 4.

Figure 4: Setup to calculate the relative orientation error for a garment-attached acceleration sensor (right) relatively to a reference sensor (left) during the execution of postures. The position of both sensors is marked with white circles.

A set of ten postures that is frequently used in shoulder and elbow rehabilitation was selected to obtain orientation errors and validate the error model as detailed in Section 4.3. Figure 5 presents all included postures. Seven participants (3 female, 4 male, aged 20 to 35 years) performed the postures in three exercise repetitions. We included participants with body heights between 163 cm and 183 cm to analyze the effect of garment fitting on the standard deviation of orientation error.

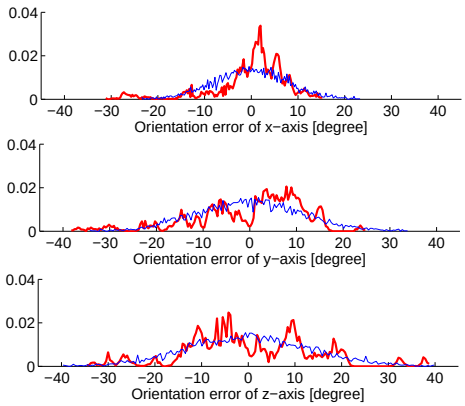

Figure 6: Orientation error distributions expressed as angular deviation for the forearm acceleration sensor axes of one participant. Red bold lines indicate the sampled distributions, blue lines show the distributions of generated sensor data using estimated Gaussian parameters.

From the recorded data we calculated angular deviation between garment-attached and reference sensors for each axis. Error models were estimated from histograms of the angular deviations. Figure 6 shows sample histograms for each acceleration sensor axis for the forearm position of one participant.

An estimation of the Gaussian distribution parameters (mean, standard deviation) was performed using a maximum likelihood estimation with a confidence interval of 5%. Table 2 summarizes standard deviations of garment-related orientation errors for each sensor (averaged over three axes).

For the forearm we obtained standard deviations of 8.4°, 14.2°, and 15°for x-, y-, and z-axis (mean: 12.5°). Large errors for y- and z-axis can be explained by orientation errors due to twists of the garment around the forearm. As acceleration sensors x-axes pointed along the forearm, this axis was insensitive to garment twists. For the upper arm, we observed standard deviations of 8.8°on average. In our ex-

Digital Object Identifier: 10.4108/ICST.BODYNETS2009.5977
http://dx.doi.org/10.4108/ICST.BODYNETS2009.5977

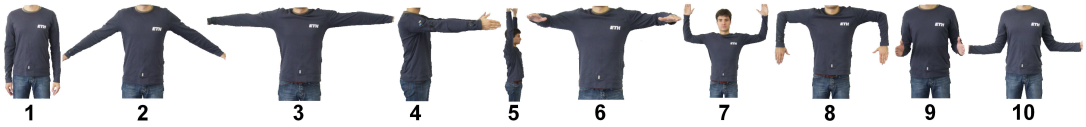

Figure 5: All ten shoulder rehabilitation postures considered in the study. The participant is wearing the SMASH system [7].

Table 2: Standard deviations (SD) of garment-related orientation errors (average over 3 axes).

Participant #	Gender [m/f]	Body height [cm]	SD upper arm [°]	SD forearm [°]
1	f	163	10	17
2	f	170	9	10.8
3	f	172	9.4	13.3
4	m	173	9.1	14.7
5	m	180	7.7	7.3
6	m	182	7.5	10
7	m	183	9.4	7
Average			8.8	12.5

perimental data the acceleration sensor placed at the upper arm was less affected by garment-related orientation errors than the forearm sensor. We expect that the reduced error at the upper arm can be explained by the garment fixation through shoulder and torso.

In Section 4.1 we presented our hypothesis that the standard deviation of orientation errors is related to garment fitting. Hence, the less tight a garment fits, the higher are orientation errors. This could be confirmed from our experimental data from participants of different body heights. Nevertheless, the garment selected for SMASH in this analysis, was designed for wearer of a body height between 177 cm and 184 cm, according to the manufacturer fitting guide. We observed in our results that participants that did not fit the manufacturer guide obtained larger standard deviations, than those who fell into the specified body height range. Figure 7 shows the standard deviations for all participants considered in our experiment. The box-plots indicate standard deviation of orientation errors for both considered sensors with 3 axes each.

4.3 Error model validation

The ability of the implemented modeling framework to simulate the orientation errors of garment-attached sensors was analyzed using the set of ten rehabilitation postures introduced in Section 4.2. For this purpose we described all postures by according joint angle configurations in our body-sensor model. Table 3 summarizes the exact configurations for all ten postures. User-specific orientation error models were derived from the posture set. Subsequently, we simulated postures for upper arm and forearm.

We compared the posture classification performance of our model-based sensor data simulation to the classification performance of actual sensor data. Ideally, posture classification using the generated sensor data would resemble the same classifier confusion and classification accuracies as actual sensor data.

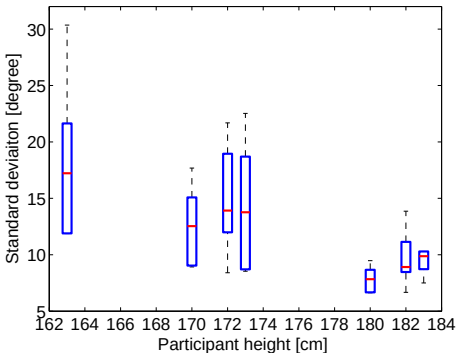

Figure 7: User-specific box-plots of the orientation error's standard deviation. The graphic indicates lower standard deviations for participants with a perfect fitting of the used SMASH garment ($177\,cm \leq height \leq 184\,cm$).

Table 3: Joint angle configurations for ten simulated rehabilitation postures (compare Figure 5).

Posture #	Should. flex./exten. [rad]	Should. adduc./abduct. [rad]	Should. in./ex. rotat. [rad]	Elbow flex./exten. [rad]	F.arm pron./supin. [rad]
1	0	0	$-\pi/2$	$10\pi/180$	$\pi/2$
2	0	$40\pi/180$	$-\pi/2$	0	$\pi/2$
3	0	$\pi/2$	$-\pi/2$	0	$\pi/2$
4	$\pi/2$	$\pi/2$	$-\pi/2$	0	0
5	0	π	$-\pi$	0	0
6	0	$\pi/2$	$-\pi/2$	$\pi/2$	$\pi/2$
7	0	$\pi/2$	$-\pi$	$\pi/2$	$\pi/2$
8	0	$\pi/2$	0	$\pi/2$	$\pi/2$
9	0	0	$-\pi/2$	$\pi/2$	$\pi/2$
10	0	$15\pi/180$	$-\pi$	$\pi/2$	$-\pi/2$

For each participant we simulated the posture set with the modulated orientation error model to generate train- and test data used for classification. For this comparison, we generated the same amount of training and testing set data as actual sensor data available for classification. We confirmed that these sample amounts have a Gaussian distribution using the Kolmogorov-Smirnov-Test with a confidence interval of 5%. A nearest class centroid-algorithm (NCC) was used to test user-specific classification performance for simulated and actual data evaluations. In both cases evaluation procedure was the same.

Classification was performed using a three-fold cross-validation scheme, aligned to the three exercise repetitions performed in the experiment. The three sensor signals of acceleration

Digital Object Identifier: 10.4108/ICST.BODYNETS2009.5977
http://dx.doi.org/10.4108/ICST.BODYNETS2009.5977

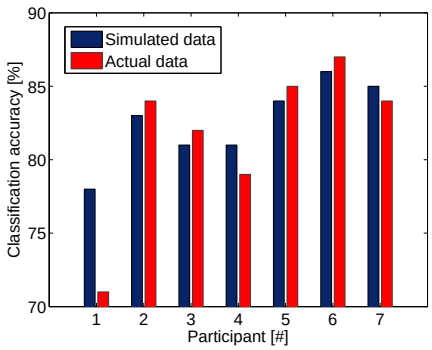

Figure 8: User-specific classification performances for all participants, using simulated and actual data.

sensors at the upper arm and forearm were used as feature input (at all 6 features) for the NCC algorithm. The class-normalized accuracy was computed from the classifier output.

Figure 8 shows the classification performances for simulated and actual data evaluations. In comparison, both evaluations obtained similar accuracies, ranging between 70% and 86%. The relative error between classification accuracies using simulated and actual data is 2.6% (SD:±3.2%). Moreover, the results show that performances have the same tendencies with respect to the participant body heights. For participants 5–7 that fell into the garment fitting specification, accuracies close to 85% were observed.

To obtain more detailed insight into classifier performances, we compared confusion matrices for both evaluations. The confusion performance confirmed the similar performance for simulation and actual sensor data. Figure 9 shows classifier confusion matrices for both evaluations for one participant (body height: 183 cm).

The simulation using generated data predicted major confusion of posture classes 3 and 6, as well as minor confusion of classes 9 and 10. Our evaluation using recorded sensor data showed only minor confusions of class 3 and 6, as well as 9 and 10. In both cases of confusions the result of generated and recorded sensor data coincided. Both identified confusions occur due to incomplete orientation information of the acceleration-based gravity sensing approach. Nevertheless, precise quantity of confusions could not be predicted. This result was confirmed for all participants, however confusions become more dissimilar with decreasing body height. For participant 1 (body height: 163 cm), our simulation correctly predicted confusions of classes 3 and 6, as well as classes 9 and 10. However, it additionally predicted a false-positive minor confusion of classes 1 and did not predict minor confusion of classes 6 and 8, which was observed in actual data. We conclude that prediction performance of the simulation decreases with large garment orientation errors.

Our validation of the body-sensor model in combination with the orientation error model showed similar classifier accuracies and classifier confusions as achieved by using actual data. We concluded that our error model can be used to estimate classifier performance. Moreover, simulation allows a predictive identification of postures that are confused by using garment-attached sensors.

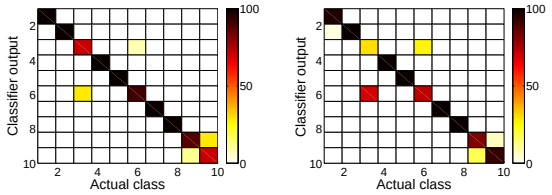

(a) Actual data (b) Simulated data

Figure 9: Comparison of confusion matrices for classifications using actual recorded and simulated data.

5. SENSOR-GARMENT SIMULATION

We utilized the body-sensor and orientation error models to simulate garment-related influences on classification performance. The models allow us to simulate the impact of particular orientation errors on the classifier performance and, consequently, to predict effects for potential fitting configurations. We deployed the same set of ten rehabilitation postures in this evaluation, as detailed before in Section 4.2 and shown in Figure 5.

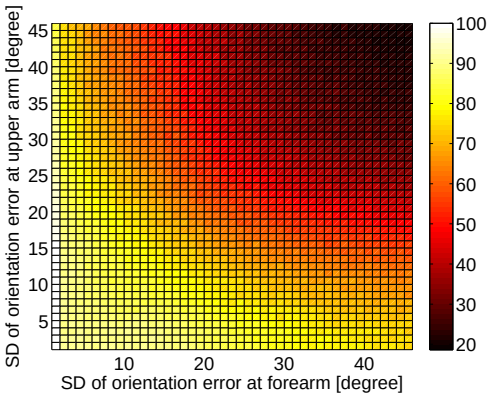

Figure 10: Classification accuracy using simulated acceleration sensor data for the upper arm and forearm. For each sensor a garment-related orientation error between 0°and 45°SD was simulated.

In this simulation, we analyzed the influence of orientation errors on the upper arm and forearm on the classification result. For both sensors, the orientation error was modeled by a Gaussian distribution with a variable standard deviation of 0°to 45°. According to Table 2 a simulated orientation error of 45°corresponds to approximately five times the observed orientation error on the upper arm and four times of the observed orientation error at the lower arm.

To evaluate classification performances we used the NCC algorithm. The NCC was trained using 500 generated samples. Performance was evaluated using another 250 gen-

Digital Object Identifier: 10.4108/ICST.BODYNETS2009.5977
http://dx.doi.org/10.4108/ICST.BODYNETS2009.5977

erated samples. Again, we confirmed that these sample amounts have a Gaussian distribution using the Kolmogorov-Smirnov-Test.

In Section 4.2 we observed that the x-axis of a forearm acceleration sensor is less affected by orientation errors. However, for this evaluation we assume a similar noise for all sensor axes of the upper arm acceleration sensor and forearm sensors respectively.

Figure 10 shows simulated classification accuracies of the ten modeled rehabilitation postures. The plot indicates that a reliable distinction of all classes is feasible if standard deviations are zero. That would be the case if sensors are directly attached to the body skin or tight fitting textiles. Moreover, the simulation shows that classification performance remains high if the standard deviation for the forearm is zero, while the standard deviation at the upper arm is less than approximately 20°. In Table 2 we estimated a mean standard deviation of 8.8°for the upper arm. Hence, for a reliable discrimination for our posture set, the forearm acceleration sensor could be fixed, while using a garment-attached acceleration sensor at the upper arm.

Figure 10 indicates that stable classification accuracies of more than 80% are obtained, if both sensors show a standard deviation of less than 20°. Our estimated standard deviations are below this bound, hence we expect a slightly imperfect but robust classification performance for the considered posture set.

6. ADDITIONAL SENSOR MODALITIES

We extended the body-sensor model to investigate potential performance improvements by adding a further sensor modality. Using the approach presented in Section 3.2 we modeled magnetic field sensors. The combination of acceleration and magnetic field sensors provide complete 3-dimensional orientation of a sensed body segment. This additional information could help to compensate orientation errors when provided to a classifier, and consequently improve overall classification performance.

In our simulation approach we assumed that both sensor modalities are integrated into one inertial sensing unit. Consequently, we assumed the same orientation error for the magnetic field sensors, as added for accelerometers. One virtual inertial sensing unit was simulated at to the upper arm and one at the forearm. Unlike acceleration sensing units, off-the-shelve magnetic field sensors show measurement inaccuracies of up to 5°. Moreover, the magnetic field is distorted in the presence of large metal objects. Those sensors-specific characteristics can be considered in an additional sensor error model, if required.

Figure 11 shows the result of our simulation for the inertial sensor units. The plot shows that classification accuracies increased, compared to an exclusive use of acceleration sensors. To visualize the improvements obtained by including magnetic field sensors in our simulation, we calculated the difference of both simulation maps. The result is shown in Figure 12. As our simulation shows, garment-attached sensors can be affected by a Gaussian noise with a standard deviation of up to 25°on both body segments and still obtain perfect posture discrimination. Moreover, the results indicate different tolerances of the classifier to simulated errors. For our selected posture set, results are predominantly affected by orientation errors of the forearm sensing unit. Classification performance was less disturbed by orientation errors of sensing units attached to the upper arm.

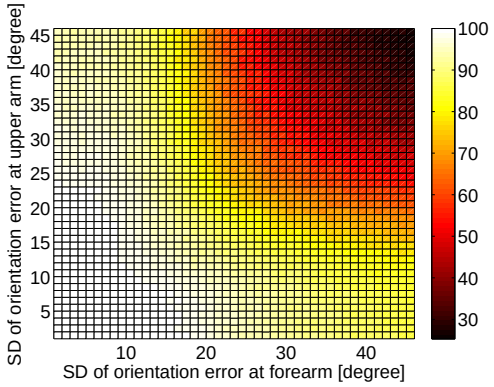

Figure 11: Simulation of classification accuracies using virtual acceleration and magnetic field sensors with garment-related orientation error of 0°to 45°SD. An inertial unit containing one of each sensor modality was simulated at the upper arm and one at the forearm.

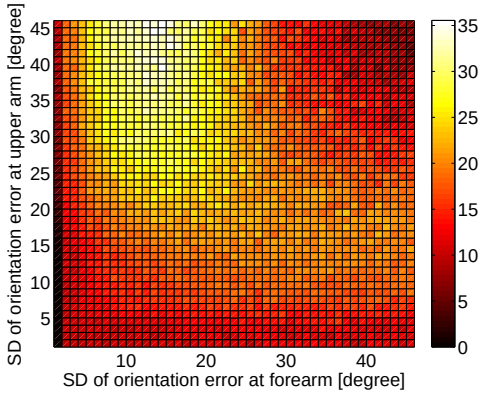

Figure 12: Difference map showing the increase in classification accuracy when magnetic field sensors are added as additional sensing modality at upper arm and forearm.

Magnetic field sensors lead to an increase in accuracy of about 18%. A particular large increase in accuracy of 35% was observed for large orientation errors at the upper arm (at 45°), and approximately 12°at the forearm. If acceleration sensors were used exclusively, the classifier performance degraded even for low orientation errors at the forearm (see Fig. 10). However, magnetic field sensors can provide a more robust basis for classification that even allow small orientation errors at the forearm while still achieving perfect classification.

Digital Object Identifier: 10.4108/ICST.BODYNETS2009.5977
http://dx.doi.org/10.4108/ICST.BODYNETS2009.5977

7. CONCLUSION AND FURTHER WORK

In this work we presented a novel approach to model body postures and orientation errors that originate from garment alignment changes. In particular, we targeted an analysis of garment fitting based on garment-related orientation errors. We implemented the models using a two-step approach. Firstly, we built a body-sensor model that allowed a flexible description of body postures for upper limbs and simulation of sensor modalities. Secondly, we approximated an orientation error model from experimental data. In our evaluations, we focused on simulating rehabilitation postures that are frequently used in shoulder and elbow exercises.

Our modeling approach showed low errors compared to experimental acceleration sensor data of the rehabilitation postures. In our validation for the model, we observed an relative error of 2.6% between posture classification results. We concluded that the orientation error modeling provides a metric to estimate garment fitting for posture recognition tasks.

Our further simulations targeted a prediction of posture recognition performance for varying orientation errors. The models allow us to estimate robustness of a configuration by alternating garment fitting parameters. Moreover, our approach is extendable to further sensor modalities, such as a magnetic field sensor. We demonstrated that this additional modality improves classification performance by 18%. The simulation provided a rapid and detailed insight into particular gains that could be obtained with such a modality.

In our further work, we plan expand our simulations to additional sensing modalities and study the compensation of orientation errors due to garment fitting in further detail.

8. REFERENCES

[1] T. Barker, C. Kirtley, and J. Ratanapinunchai. Calculation of multi-segment rigid body joint dynamics using matlab. In *Proceedings of the Institution of Mechanical Engineers, Part H: Journal of Engineering in Medicine*, pages 483–487, 01 1997.

[2] L. Buechley and M. Eisenberg. Fabric PCBs, electronic sequins, and socket buttons: Techniques for e-textile craft. *Personal and Ubiquitous Computing*, 2007. Published online.

[3] P. Corke. A robotics toolbox for MATLAB. *IEEE Robotics and Automation Magazine*, 3(1):24–32, March 1996.

[4] J. Denavit and R. S. Hartenberg. A kinematic notation for lower-pair mechanisms based on matrices. *Trans ASME J. Appl. Mech*, 23:215–221, 1955.

[5] J. Edmison, D. Lehn, M. Jones, and T. Martin. E-textile based automatic activity diary for medical annotation and analysis. In *BSN 2006: Proceedings of the International Workshop on Wearable and Implantable Body Sensor Networks*, pages 131–134, April 2006.

[6] F. Gemperle, C. Kasabach, J. Stivoric, M. Bauer, and R. Martin. Design for wearability. In *ISWC 1998: Proceedings of the IEEE International Symposium on Wearable Computers*, 1998.

[7] H. Harms, O. Amft, D. Roggen, and G. Tröster. SMASH: A distributed sensing and processing garment for the classification of upper body postures. In *BodyNets 2008: Proceedings of the Third International Conference on Body Area Networks*. ACM press, March 2008.

[8] H. Harms, O. Amft, and G. Tröster. Influence of a loose-fitting sensing garment on posture recognition in rehabilitation. In *BioCAS 2008: Proceedings of the Biomedical Circuits and Systems Conference*, 0 2008.

[9] H. Junker, P. Lukowicz, and G. Troster. Padnet: Wearable physical activity detection network. In *ISWC 2003: Proceedings of the 7th International Symposium on Wearable Computers*, 2003.

[10] J. Knight, D. Deen-Williams, T. Arvanitis, C. Baber, S. Sotiriou, S. Anastopoulou, and M. Gargalakos. Assessing the wearability of wearable computers. *Wearable Computers, 2006 10th IEEE International Symposium on*, pages 75–82, Oct. 2006.

[11] K. Kunze and P. Lukowicz. Dealing with sensor displacement in motion-based onbody activity recognition systems. In *UbiComp '08: Proceedings of the 10th international conference on Ubiquitous computing*, pages 20–29, NY, USA, 2008. ACM.

[12] E. Lou, M. J. Moreau, D. L. Hill, V. J. Raso, and J. K. Mahood. Smart garment to help children improve posture. *Engineering in Medicine and Biology Society, 2006. EMBS '06. 28th Annual International Conference of the IEEE*, pages 5374–5377, 30 2006-Sept. 3 2006.

[13] S. Mann. Smart clothing: the shift to wearable computing. *Communications of the ACM*, 39(8):23–24, Aug. 1996.

[14] C. Mattmann, O. Amft, H. Harms, G. Tröster, and F. Clemens. Recognizing upper body postures using textile strain sensors. In *ISWC 2007: Proceedings of the 11th IEEE International Symposium on Wearable Computers*, pages 29–36. IEEE Press, October 2007. Recipient of the IEEE ISWC 2007 Best Paper Award.

[15] M. W. Spong. *Robot Dynamics and Control*. John Wiley & Sons, Inc., New York, NY, USA, 1989.

[16] A. Tilley. *The measure of man and woman : human factors in design*. Whitney Library of Design, 1. print edition, 1993.

[17] A. Tognetti, F. Lorussi, M. Tesconi, R. Bartalesi, G. Zupone, and D. De Rossi. Wearable kinesthetic systems for capturing and classifying body posture and gesture. *Engineering in Medicine and Biology Society, 2005. IEEE-EMBS 2005. 27th Annual International Conference of the*, pages 1012–1015, 2005.

[18] K. Van Laerhoven, A. Schmidt, and H.-W. Gellersen. Multi-sensor context aware clothing. *Wearable Computers, 2002. (ISWC 2002). Proceedings. Sixth International Symposium on*, pages 49–56, 2002.

Digital Object Identifier: 10.4108/ICST.BODYNETS2009.5977
http://dx.doi.org/10.4108/ICST.BODYNETS2009.5977